Multiple Fano Resonances in Plasmonic Heptamer Clusters Composed of Split Nanorings

Shao-Ding Liu,[*,†,‡,§] Zhi Yang,[†,‡] Rui-Ping Liu,[†,‡] and Xiu-Yan Li[†,‡]

[†]Key Lab of Advanced Transducers and Intelligent Control System of Ministry of Education, Taiyuan University of Technology, Taiyuan 030024, P. R. China, [‡]Department of Physics and Optoelectronics, Taiyuan University of Technology, Taiyuan 030024, P. R. China, and [§]Department of Physics, Wuhan University, Wuhan 430072, P. R. China

ABSTRACT

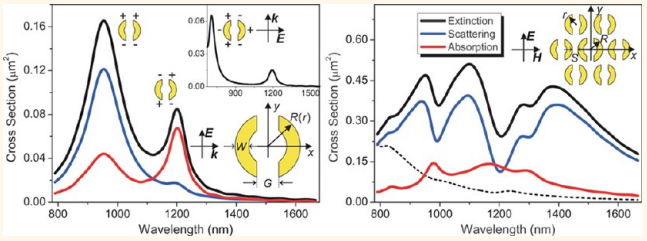

Fano resonances in plasmonic nanostructures are important for plasmon line shaping. Compared to a single Fano resonance, multiple Fano resonances can modify plasmon lines at several spectral positions simultaneously, but they often suffer from weak modulation depths. In this paper, plasmonic heptamer clusters comprising split nanorings are designed to form multiple Fano resonances. Three prominent Fano resonances are observed in the spectra due to the formation of multiple narrow subradiant resonances, and the multiple Fano resonances can be switched on and off by adjusting the polarization direction. Particularly, by modifying the geometry parameters, there is a large tunability of the modulation depth of each Fano resonance. Heptamer clusters comprising split nanorings are highly suitable for plasmon line shaping, and it is expected that they are useful for multiwavelength biosensing and surface-enhanced Raman scattering.

KEYWORDS: surface plasmon · metallic nanostructure · Fano resonances · oligomer cluster · dark mode · split nanoring

The collective oscillations of the conduction electrons of a metallic nanoparticle (NP) can result in localized surface plasmon resonances (LSPRs), which depend sensitively on the NP's size, shape, and surrounding medium.[1,2] In hybrid structures of NPs, surface plasmon (SP) coupling can create regions of concentrated fields, which are the so-called "hot-spots". Many applications using LSPRs have been demonstrated based on these properties. Fano resonances in metallic nanostructures caused by the interaction of narrow dark modes with broad bright modes have gained much attention in recent years.[3−5] The coupling can lead to a plasmon-induced transparency for strong interactions and near-degenerate levels.[6] Traditionally Fano resonances were considered mostly in quantum systems,[7] but they have been realized in different nanostructures, such as dolmen nanostructures,[6,8] ring-disk nanocavity,[9] nanocross,[10] mismatched NP dimer,[11−14] heterodimer,[15−17] nanodisk with symmetry breaking,[18] nanoshell,[19,20] NPs coupling with substrate,[21−23] and NP oligomer.[24−27] NP oligomer is one of the most promising nanostructures to form Fano resonances. For example, a plasmonic heptamer consists of a bright superradiant mode and a dark subradiant collective mode. The spectral overlap and destructive interference of these two modes leads to the formation of the Fano resonance.[24] By adjusting the geometry of NP oligomers, a plasmonic pentamer,[28,29] quadrumer,[30−32] and trimer[33,34] have been used to form Fano or Fano-like resonances too. Reported results also show that by modifying the interparticle separation, relative particle size, or breaking the symmetry of a plasmonic oligomer, there is a large tunability of the modulation depth as well as the spectral position of the Fano resonance.[35−38]

Owing to their asymmetric line shape, sharp resonance, and sensitivity to a variety of parameters, Fano resonances are very useful for plasmon line shaping, and a lot of applications have been developed based on this property. For example, radiative damping at the spectral position of the Fano resonance can be effectively suppressed, leading to a narrow line width. As a result, the figure of merit (FoM) that be used to characterize the biosensing performance can be significantly enlarged.[39−43] Fano resonances are also useful for surface enhanced Raman scattering (SERS). The field enhancement needs to be simultaneously

* Address correspondence to liushaoding@tyut.edu.cn.

Received for review April 18, 2012 and accepted June 10, 2012.

Published online June 10, 2012
10.1021/nn3017052

enhanced at both the pump wavelength and the Stokes-shift Raman wavelength to further boost the signal intensity of SERS. There is strong field enhancement at the spectral position of Fano resonance, the energy of incident light can be effectively confined around the NPs due to the strong absorption, and Fano resonances are very suitable for SERS.[44−48] Besides the above applications, Fano resonances have also been used for enhanced light transmission,[49,50] slow light,[6] and classical analog of electromagnetically induced absorption (EIA).[51]

At the same time, several theories have been used to describe and explain the formation of Fano resonance. The plasmon hybridization (PH) model has been proposed to describe the plasmon response of complex nanostructures of arbitrary shape.[52] Coupling between individual plasmon modes leads to splitting of the modal energies into bonding and antibonding combinations according to the PH theory. The PH theory is a powerful tool to investigate SP interactions, and it has been widely used to help understand the generation of Fano resonances. Besides the PH theory, the emergence of Fano resonances can be well explained *via* the coupled oscillator model.[53] For Fano resonances generated in plasmonic oligomers, symmetry considerations are as important as group theory in molecular physics, and the group theory has been successfully used to understand the formation of Fano resonances.[54−56] Not long ago, a straightforward analytical formula was obtained to study Fano resonance in plasmonic nanostructures. Without the need of additional fitting parameters, it allows one to predict or reproduce the formation of Fano resonances in coupled nanostructures.[57,58]

Recently, multiple Fano resonances have gained much attention.[59] Compared to a single Fano resonance, a plasmon line can be modified at several spectral positions simultaneously for multiple Fano resonances, and it would be useful for multiwavelength SERS and biosensing. Liu *et al*. proposed and fabricated a kind of multilayer plasmonic oligomer composed of a nanorod and two nanorod dimers, which possesses two dark quadrupole modes with energy detuning, resulting in double Fano resonances in the spectra.[60,61] They showed that such a nanostructure can be used as three-dimensional plasmon rulers. Artar *et al*. designed a multilayer nanostructure consisting of coupled meta-atoms, double Fano resonances appeared corresponding to in phase and out of phase hybridized modes.[62] Consequently, they found double Fano resonances also can be formed in a hetero-oligomer structure where the multiple radiant and subradiant modes can be tailored independently, and due to its inherent asymmetry, the proposed structure can be used as an ultracompact and highly directional on-chip antenna.[63] After that, Dregely *et al*. reported that for a plasmonic oligomer cluster, multiple Fano resonances can be observed by adjusting the number of NPs or their respective arrangement.[64] With the formation of magnetic plasmons, Liu *et al*. showed that a similar NP heptamer chain can be used as low loss SP waveguiding.[65,66] Most recently, Fu *et al*. reported the formation of higher order Fano resonances in dual-disk ring nanostructures.[67]

Although multiple Fano resonances have been generated and used for certain applications, it can be found that they still suffer from weak modulation depths, that is, one or more modulation depths of the multiple Fano resonances are weak in the spectra, which is a drawback for plasmon line shaping. In this paper, we show that for a split nanoring (SNR) with two gaps, there is a small energy gap between the dark quadrupole mode and the bright dipole mode. When the SNRs are aligned together to form a heptamer, the quadrupole and dipole modes of each SNR are coupling with each other. Calculation results show that three prominent Fano resonances appear in the spectra due to the formation of multiple narrow subradiant resonances, and there is a large tunability of the modulation depth for each Fano resonance by modifying the geometry. Heptamer clusters composed of split nanorings can modify plasmon lines at several spectral positions at the same time, and they are highly suitable for plasmon line shaping.

RESULTS AND DISCUSSION

The inset of Figure 1a shows the geometry of a SNR with two gaps, where W is the width, G is the length of the two gaps, R (or r) is the outer radius, and the thickness is represented by H. The main panel of Figure 1a is the spectra of a SNR being illuminated from the side at grazing incidence, where $W = 30$ nm, $G = 30$ nm, $R = 75$ nm, $H = 40$ nm, and the refractive index of surrounding medium is $n = 1.33$. There are two resonances around 954 and 1201 nm, which are the dipole and quadrupole modes, respectively. The quadrupole resonance is a dark mode, it couples weakly to external field, and the quadrupole resonance cannot be excited under normal incident excitation. The inset of Figure 1a also shows the extinction spectrum of the SNR when the polarization is along the x axis, a resonance around 707 nm is present in the spectrum, there are six charge lobes around the SNR, and it is far away from the quadrupole mode.[42]

A plasmonic heptamer cluster comprising nanodisks (or nanospheres) is a promising structure to form Fano resonance, where the interaction between the in phase and out of phase collective dipole resonances plays a key role.[24] Because of the large energy gap between the quadrupole and dipole modes, the quadrupole resonance is far away from the superradiant bright mode of the whole structure. The quadrupole

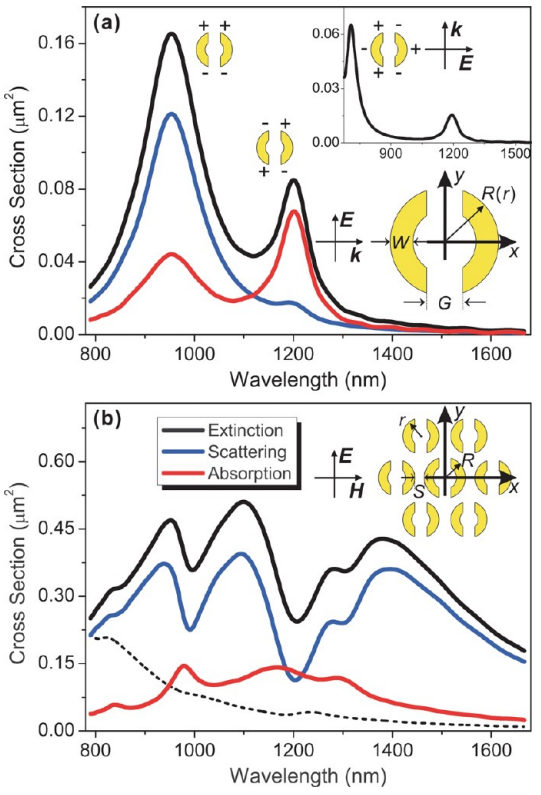

Figure 1. (a) Spectra of a SNR under oblique incident excitation, where the inset on the lower right corner represents the geometry of the SNR, the parameters used are W = 30 nm, G = 30 nm, R = 75 nm, the thickness H = 40 nm, and the refractive index of surrounding medium is n = 1.33. The inset on the upper right corner is the extinction spectrum when the polarization is along the x axis. (b) Spectra of a plasmonic heptamer cluster composed of SNRs, where the radius of center SNR and surrounding SNRs are, respectively, R = 80 nm and r = 75 nm, the separation S = 20 nm, and the dashed line is the extinction spectrum when the polarization is along the x axis.

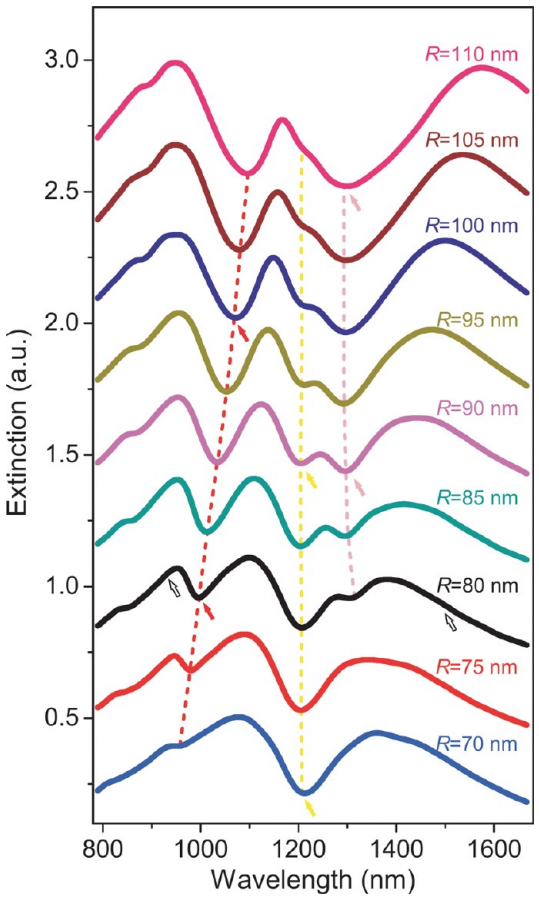

Figure 2. Extinction spectra evolution *versus* the radius of center SNR of the plasmonic heptamer clusters composed of SNRs, where the other parameters are the same as Figure 1b.

resonance of the nanodisk is also relatively weak compared with the dipole mode. As a result, the quadrupole mode contributes little to the formation of the Fano resonance.

Compared with that of a nanodisk, the quadrupole resonance of a SNR is much stronger, and there is a small energy gap between the dipole and the quadrupole modes. The quadrupole mode of SNRs or similar structures (nanorod dimers) has been widely used to form Fano resonances. Consider a plasmonic heptamer cluster as shown in the inset of Figure 1b, which is composed of SNRs. According to the PH theory, there is also a superradiant bright mode when the dipole resonances of each SNR are in phase. The quadrupole mode of the SNRs can overlap with the superradiant bright mode due to the small energy gap, which may help to form new Fano resonances. The solid lines in Figure 1b show the spectra of a heptamer cluster composed of SNRs, where the center ring R = 80 nm, the surrounding ring r = 75 nm, the separation between the center and surrounding rings S = 20 nm, and the polarization is along the y axis. Three Fano resonances are observed in the spectra, and it is noted that the fundamental Fano dip is around 1208 nm, which is almost at the same spectral position as that of the quadrupole mode of the surrounding SNRs.

The dashed line in Figure 1b is the extinction spectrum when the polarization is along x axis. As shown in the inset of Figure 1a, the resonance with six charge lobes is far away from the quadrupole mode, it cannot help to form a Fano resonance, and no Fano resonance is present in the spectrum when the polarization is along the x axis. This phenomenon implies that with the plasmonic heptamer clusters composed of SNRs, the multiple Fano resonances can be switched on and off by adjusting the polarization direction.[64]

In the following, we will show that by modifying the structure geometry, there is a large tunability of the modulation depth of each Fano resonance. Figure 2 represents the extinction spectra as a function of the size of center SNR. The overall dipole moment of the superradiant bright mode increases with an increase of R, resulting in a spectral broadening. The first Fano resonance which has the highest energy (marked with red dashed line) shifts to lower energies with

increasing R, and the modulation depth increases dramatically. The modulation depth of the second Fano resonance (marked with yellow dashed line) decreases with increasing R, and it is almost at the same spectral position. As for the third Fano resonance which has the lowest energy (marked with magenta dashed line), there is a small kink when $R < 80$ nm, the modulation depth increases with the increase of R, and a small blue shifting is also observed.

To explain the appearance of multiple Fano resonances, near-field and current density vector distributions at the spectral positions of the superradiant bright mode as well as the three Fano resonances are inspected. For the heptamer with $R = 80$ nm, Figure 3 panels a and b represent the field distributions at the structure cross section when the incident wavelengths are 940 and 1500 nm, respectively. Similarly to the case of a heptamer cluster composed of nanodisks, the dipole resonances of each SNR oscillate in phase, resulting in the bright superradiant collective mode, which has a broad line width. The sum of the dipole moments of all in phase oscillating SNR plasmons increases with increasing R, and the line width of the superradiant bright mode is broadening.

In the case of the first Fano resonance with $R = 80$ nm, near-field properties are shown in Figure 3c. For the upper and lower four SNRs, there are strong field enhancements in the two gaps, and current density vector distributions imply that there are four charge lobes around each SNR. It is the same as that of the quadrupole mode of a SNR, and there is a weak radiative damping of these SNRs. For the middle three SNRs, the dipole resonance of the center SNR oscillate out of phase with the left- and right-side SNRs, resulting in a cancellation of their dipole moments. Therefore, the radiative damping of the whole structure is weak, and the overall dipole moment decreases dramatically at this spectral position, which forms a subradiant collective mode. The subradiant mode is overlapped with the superradiant bright mode, and the destructive interference of these two modes leads to the formation of the first Fano resonance in the spectra.

It is worth noting that the heptamer cluster can be separated into two parts: part one, the upper and lower four SNRs, and part two, the middle three SNRs. As shown in Figure 3c, field enhancements at the separations between these two parts are relatively weak. The subradiant collective mode of the first Fano resonance can be viewed as an antibonding resonance according to the PH theory.

When R is enlarged to 100 nm, Figure 3d represents the near-field properties at the spectral position of the first Fano resonance. Compared with that of $R = 80$ nm, the dipole moment of the center SNR is enlarged, and the cancellation of dipole moments within the middle three SNRs becomes more effective, leading to

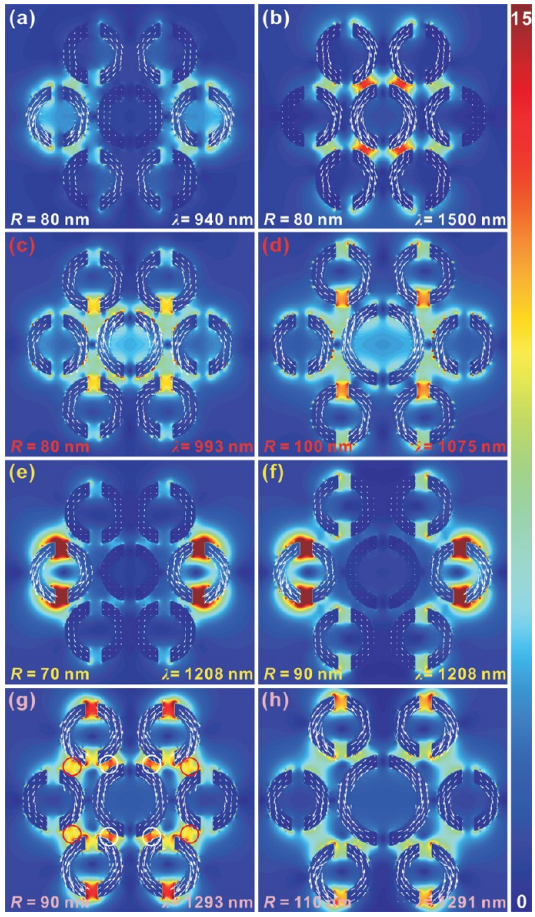

Figure 3. Field enhancement ($|E|/|E_{inc}|$) and current density vector distributions at the cross section of plasmonic heptamer clusters composed of SNRs. (a) The superradiant bright mode with $R = 80$ nm at the spectral position of $\lambda = 940$ nm and (b) $\lambda = 1500$ nm. (c) The first Fano resonance with $R = 80$ nm and (d) $R = 100$ nm. (e) The second Fano resonance with $R = 70$ nm and (f) $R = 90$ nm. (g) The third Fano resonance with $R = 90$ nm and (h) $R = 110$ nm.

a weaker radiative damping of the subradiant mode. As a result, the modulation depth of the first Fano resonance is stronger for a heptamer with larger center SNR. With the increase of R, the dipole resonance energy of the center SNR decreases, the separations between the surrounding SNRs are increasing, and the restoring force associated with the antibonding mode of the first Fano resonance is reduced. Therefore, the first Fano resonance shifts to lower energies with the increase of R.

Figure 3e shows the near-field properties of the second Fano resonance when $R = 70$ nm. There are very strong field enhancements in the two gaps of the left- and right-side SNRs, the current density vector distributions imply that it is the same as the quadrupole mode, which helps to form a new subradiant collective mode. The new subradiant mode also overlaps with the superradiant bright mode, and the destructive interference of these two modes leads to the formation of the second Fano resonance. Near-field

properties of the second Fano resonance when R = 90 nm are represented in Figure 3f. The dipole moment of the center SNR is enlarged compared with that of R = 70 nm, and the separations between the surrounding SNRs are also increased, leading to a weaker SP coupling. Therefore, the modulation depth of the second Fano resonance decreases with increasing R. The quadrupole resonance of the surrounding SNRs is the main cause of the subradiant mode of the second Fano resonance, and it is almost at the same spectral position for different clusters since the geometry of surrounding SNRs is unchanged.

The formation of the third Fano resonance also can be understood by investigating the near-field properties. Figure 3g shows the near-field and current density vector distributions of the third Fano resonance when R = 90 nm. It can be found that the current density vector distributions of each SNR are the same as the first Fano resonance, resulting in a weak radiative damping, which forms another new subradiant mode, and the third Fano resonance arises at this spectral position. But compared with that of the first Fano resonance, there are stronger field enhancements between the two parts of the cluster. According to the PH theory, the subradiant mode of the third Fano resonance can be viewed as the corresponding bonding resonance. When R is enlarged to 110 nm, near-field properties of the third Fano resonance are seen (Figure 3h). Like the first Fano resonance, the dipole moment of the center SNR is increased, and there is a more effective cancellation of the dipole moments of the middle three SNRs, which leads to an increase in the modulation depth. Since the separations between the surrounding SNRs increase with increasing R, the third Fano resonance is blue shifted because of the weaker SP interactions.

Compared to that of the first Fano resonance, the modulation depth of the third Fano resonance is much weaker when R < 90 nm. As it has been mentioned before, at the spectral position of the third Fano resonance, there are strong field enhancements between the two parts of the cluster, which would generate additional dipole moments. The current density vector distributions imply that the plasmon oscillation is out of phase between region one (marked with white circles in Figure 3g) and region two (marked with red circles in Figure 3g), and there is a cancellation of their dipole moments. But the separations of region one and region two are not equal to each other. Former studies have shown that for a NP dimer, SP coupling strength in the gap increases exponentially with the decreasing of the separation. For the same reason, the cancellation of dipole moments between these two regions is not so effective when R is small, and there is only a kink of the third Fano resonance when R < 80 nm.

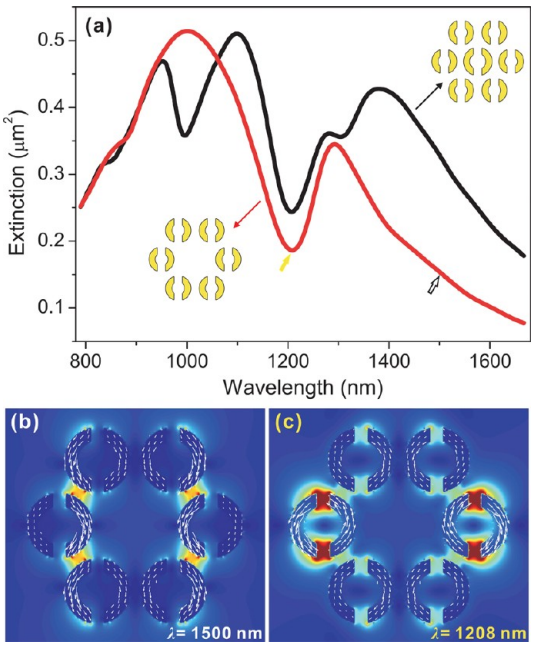

Figure 4. (a) Extinction spectrum of the cluster when the center SNR is removed (red line), and the corresponding extinction spectrum of the heptamer with R = 80 nm (black line). (c) Near-field properties at the spectral position of the superradiant bright mode, and (d) the Fano resonance of the hexamer, where the parameters used are the same as in Figure 1b.

Compared to a heptamer cluster composed of nanodisks, all of the three Fano resonances are in the near-infrared as shown in Figure 2. Since the first Fano resonance is related to the subradiant antibonding mode, which has a higher energy than the quadrupole mode of SNRs, one may expect that the first Fano resonance can be shifted to the visible by modifying the geometry parameters. Extinction spectra of the clusters with different overall size are represented in Figure S1 in the Supporting Information, the first Fano resonance is around 754 nm when the overall size is scaled down to 25% of the original structure, and due to the decrease of the radiative damping of the superradiant bright mode, the modulation depths of the Fano resonances decrease with the decrease of the overall size.

The above discussions have shown that the first and the third Fano resonances are related to the center SNR, and the surrounding SNRs play the key roles for the formation of the second Fano resonance. To confirm these conclusions, the optical response of a cluster without a center SNR is investigated. The red line in Figure 4a is the extinction spectrum of the cluster without a center SNR. Compared with that of the heptamer (black line), there is only one Fano resonance around 1208 nm, which is at the same spectral position of the second Fano resonance. The first and the third Fano resonances are not observed in this case because of the absence of the center SNR. Figure 4b shows the near-field properties of the bright superradiant

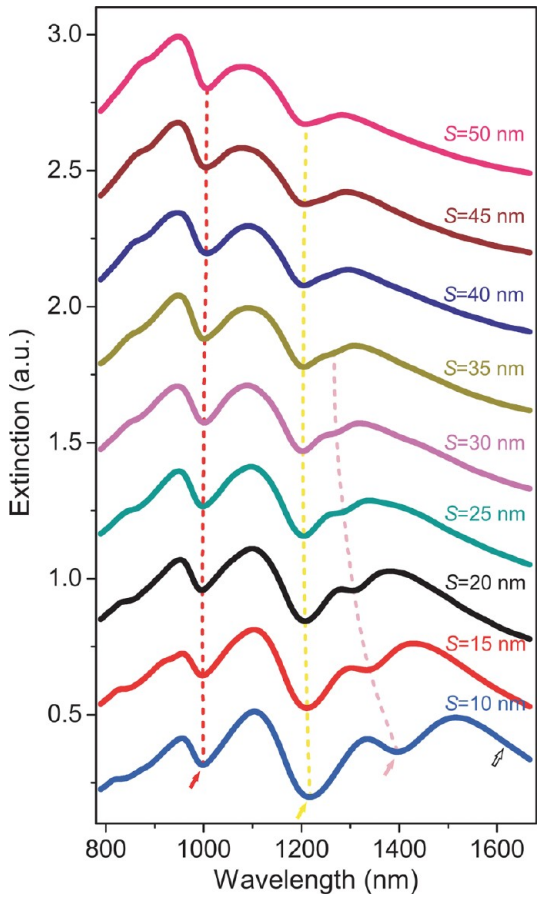

Figure 5. Extinction spectra of plasmonic heptamer clusters composed of SNRs as a function of the separation *S*, where the other parameters are the same as Figure 1b.

resonance at 1500 nm, where dipole resonances of each SNR oscillate in phase. The overall dipole moment is reduced when the center SNR is removed, and the line width of the superradiant mode is narrower than that of the heptamer. In Figure 4c, near-field distributions at the spectral position of the Fano resonance are plotted. As the second Fano resonance of the heptamer, the quadrupole mode of the surrounding SNRs overlaps with the superradiant mode, leading to the formation of the Fano resonance.

Another possibility to modify the modulation depths of the multiple Fano resonances is by adjusting the separation *S*. Figure 5 shows the relationship between the extinction spectra and *S* of the heptamer cluster. The bright superradiant mode is broadening with the decrease of *S*. The first Fano resonance slightly shifts to lower energies with the increase of *S*. The second Fano resonance is almost at the same spectral position, but the modulation depth decreases dramatically with the increase of *S*, and a decreasing symmetry of the second Fano resonance is also observed in the spectra. For the third Fano resonance, it is blue shifting with the increase of *S*, the modulation depth is decreasing, and there is only a kink when $S > 30$ nm.

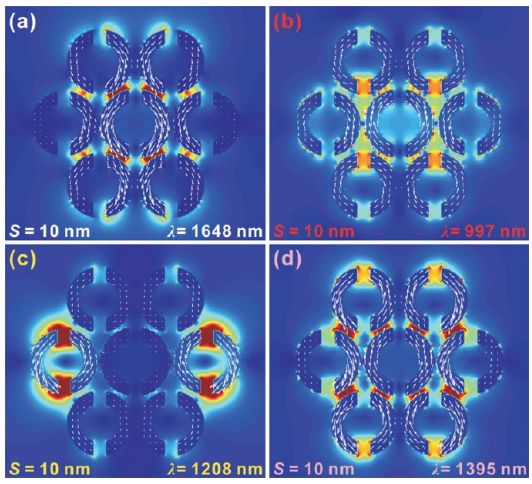

Figure 6. Near-field properties of (a) the superradiant bright mode, (b) the first, (c) the second, and (d) the third Fano resonances of the heptamer with $S = 10$ nm.

Near-field properties of the heptamers with different *S* also will be inspected to understand the underlying physics of the changes of spectral features. Figure 6a shows the near-field distribution of the heptamer with $S = 10$ nm when $\lambda = 1648$ nm. Dipole resonances of each SNR oscillate in phase, resulting in the superradiant bright mode. When *S* is enlarged, there are weaker SP interactions between these SNRs, and the overall dipole moment of the whole structure is decreased. Consequently, the superradiant bright mode shifts to higher energies, and the corresponding line width becomes narrower. The near-field properties of the first Fano resonance around 997 nm are represented in Figure 6b. Owing to the antibonding resonance of the subradiant mode of the first Fano resonance, field enhancements in the separations are weak, and the restoring force of the subradiant mode decreases with the increase of *S*. Just like the antibonding resonance of a nanorod dimer,[68] the subradiant mode is red shifting with the increase of *S*, and the first Fano resonance shifts to lower energies. With the blue shifting of the superradiant bright mode, the energy gap between the superradiant and subradiant mode of the first Fano resonance is decreased, and the modulation depth of the first Fano resonance is not changed much. Near-field properties of the second Fano resonance are represented in Figure 6c. It has been noted that the second Fano resonance is related to the quadrupole mode of the surrounding SNRs. Since the geometry of the surrounding SNRs is unchanged, the second Fano resonance is at the same spectral position for different *S*. On the other hand, SP interactions between the SNRs decrease with the increase of *S*, leading to a weaker SP coupling. As a result, the modulation depth of the second Fano resonance decreases with the increase of *S*. Figure 6d represents the near-field properties of the third Fano resonance when $S = 10$ nm. Compared with that of the first Fano

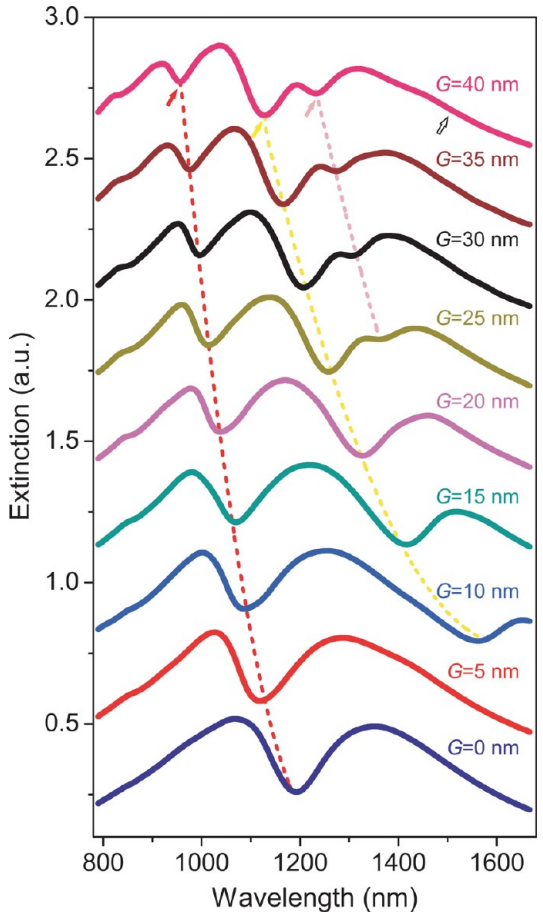

Figure 7. Extinction spectra of plasmonic heptamer clusters composed of SNRs *versus* the gap size *G* of SNRs, where the other parameters are the same as defined in Figure 1b.

resonance caused by the antibonding mode, there are stronger field enhancements in the separations caused by the bonding mode of the third Fano resonance. SP interactions decrease with the increase of *S*, leading to the blue shift of the third Fano resonance. At the same time the superradiant bright mode is blue shifting, the radiative damping of the superradiant bright mode decreases dramatically at the spectral position of the bonding resonance. Therefore, the modulation depth of the third Fano resonance decreases with the increase of *S*, and there is only a kink for a large separation.

The optical responses of SNRs can be affected by the gap size *G* significantly, so one can expect that the spectral feature of the heptamer can be modified by *G*. Figure 7 shows the extinction spectra evolution *versus* *G*. All of the three Fano resonances shift to lower energies with the decrease of *G*, and the second Fano resonance has the most prominent red shifting. The modulation depth of the first Fano resonance increases with the decrease of *G*, while the symmetry of the spectral feature increases. On the other hand, the modulation depths of the second and the third Fano resonances decrease with the decrease of *G*, the

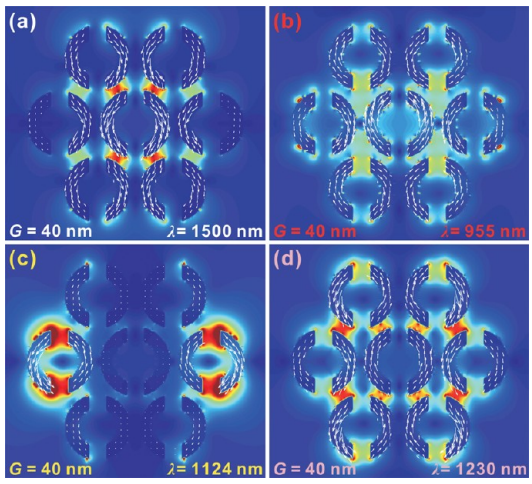

Figure 8. Near-field properties of (a) the superradiant bright mode, (b) the first, (c) the second, and (d) the third Fano resonances of the heptamer with *G* = 40 nm.

second Fano resonance is not visible in the spectral range when $G < 10$ nm, and there is only a kink for the third Fano resonance when $G < 25$ nm. Especially, it is found that the first Fano resonance evolves into the only one prominent Fano resonance when $G = 0$, which is in accordance with that of a plasmonic heptamer composed of nanodisks.

Near-field properties of the heptamer with $G = 40$ nm are plotted in Figure 8 to explain the spectral differences. The superradiant bright mode shown in Figure 8a is causing by the collective in phase dipole resonance of the SNRs. There is a minor influence to the dipole resonance of a SNR by modifying *G*, so the line width as well as the spectral position of the superradiant bright mode is not changed much. SP interactions in the two gaps of a SNR are stronger for a smaller *G*, and it can be expected that the quadrupole mode of the SNRs is red shifting with the decreasing of *G*. The above studies have shown that the three Fano resonances are related to the quadrupole mode of the surrounding SNRs. As a result, all of the three Fano resonances red shift with the decrease of *G* according to the PH theory. On the other hand, at the spectral position of the first Fano resonance shown in Figure 8b, the charge distributions of the upper and lower SNRs are similar as the quadrupole mode, but field enhancements in the two gaps of a SNR are not equal to each other. This phenomenon reveals that the cancellation of the dipole moments in the two gaps is not as effective as the quadrupole mode of a SNR. With the decrease of *G*, the cancellation of dipole moments becomes more effective. At the same time, the energy gap between the subradiant antibonding mode and the superradiant bright mode decreases, leading to the enhancement of the modulation depth of the first Fano resonance, and it evolves into a symmetric Fano line as that of a heptamer composed of nanodisks when $G = 0$. The second Fano resonance represented in Figure 8c

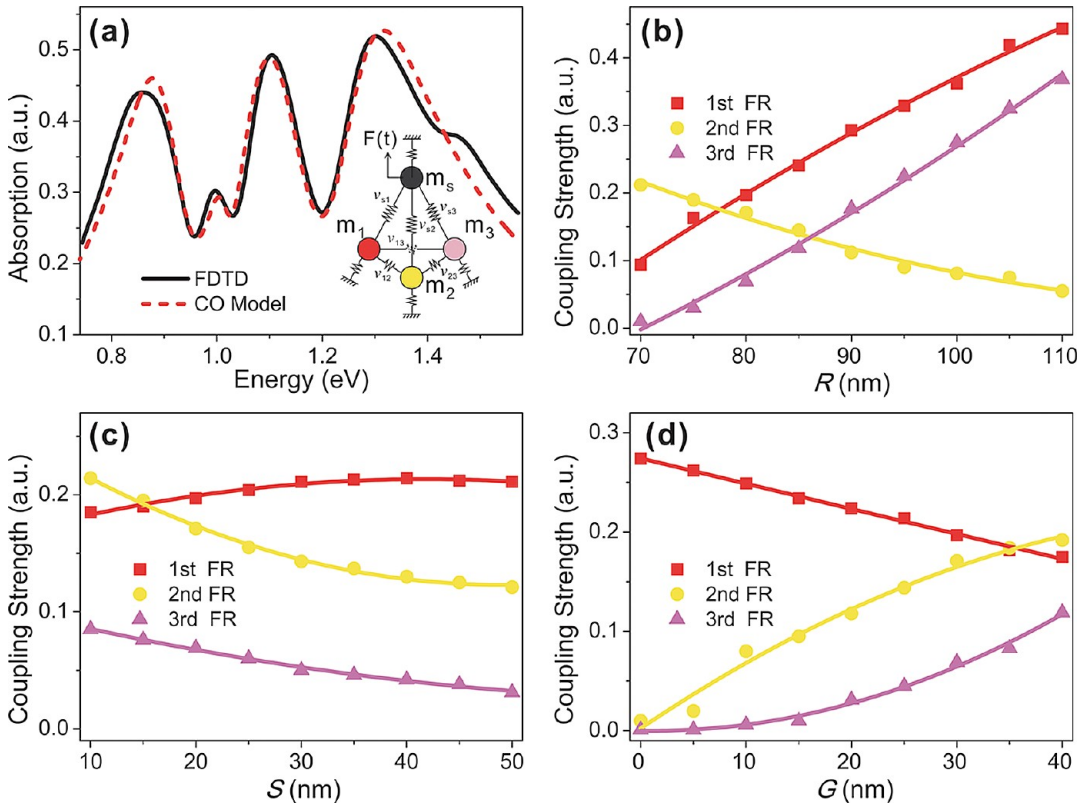

Figure 9. Simulation results of the coupled oscillator model. (a) Comparison between the extinction spectrum calculated with FDTD (black solid line) and the absorbed power by oscillator $|s\rangle$ by using the coupled oscillator model (red dashed line), where $R = 90$ nm. (b) The simulated coupling strengths *versus* the center ring radius R, (c) the separation S, and (d) the gap size G. The other parameters are the same as in Figure 1b.

red shifts dramatically with the decrease of G, which means the quadrupole mode of the surrounding SNRs shifts toward to the tail of the superradiant bright resonance, at where the radiative damping of the superradiant mode is weak, resulting in a decrease of the modulation depth of the second Fano resonance. When $G < 10$ nm, the quadrupole mode is out of the spectral range, and the second Fano resonance is not visible in the spectra. For the same reason, at the spectral position of the subradiant bonding mode of the third Fano resonance as shown in Figure 8d, radiative damping of the superradiant resonance decreases with the decrease of G, leading to the decrease of the modulation depth of the third Fano resonance.

To quantitatively characterize the coupling strengths between the superradiant and subradiant modes of the three Fano resonances, a mechanical model consisting of four coupled oscillators as shown in the inset of Figure 9a is used to study the formation of the multiple Fano resonances.[19,53] All of the mass values are supposed to be 1, and only oscillator $|s\rangle$ is driven by a harmonic force as that of the optical excitation of the superradiant bright mode. The three subradiant modes related to the multiple Fano resonances are represented by, respectively, oscillator $|1\rangle$, $|2\rangle$, and $|3\rangle$. They are only excited because of the coupling with oscillator $|s\rangle$, and there are also weak couplings between oscillators $|1\rangle$, $|2\rangle$, and $|3\rangle$. The red dashed line in Figure 9a is the calculation result of the absorbed power by oscillator $|s\rangle$ from the external force, and it agrees well with the extinction spectrum. Figure 9b shows the relationships between the simulated coupling strengths and the radius R of the center SNR. The coupling strengths of the first and the third Fano resonances increase dramatically with the increase of R, while the coupling strength of the second Fano resonance decreases. The simulation results are in accordance with the variations of the modulation depths of the three Fano resonances calculated with FDTD. The evolutions of the coupling strengths of the multiple Fano resonances with the separation S are represented in Figure 9c. There is a minor change of the coupling strength of the first Fano resonance, and the modulation depth is not changed much as we have observed before. The coupling strengths of the second and the third Fano resonances decrease with the increase of S, leading to the decrease of the modulation depths. Figure 9d shows the variations of the coupling strengths against the gap size G. The same as the extinction spectra, the coupling strength of the first Fano resonance decreases with the increase of G, while the coupling strengths of the other two Fano resonances increase. Please refer to the Supporting Information for the motion equations, parameters

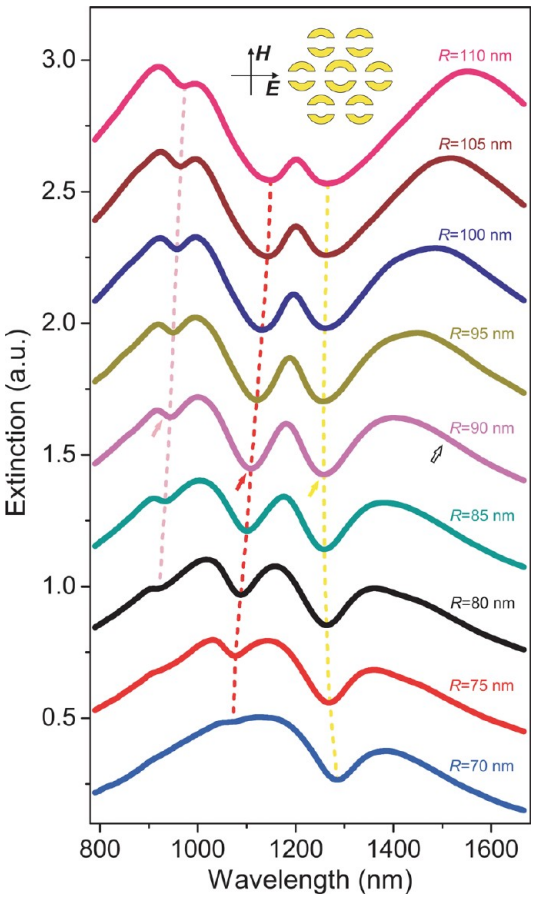

Figure 10. Extinction spectra *versus* the radius of center SNR for plasmonic heptamer clusters composed of SNRs with the new arrangement as shown in the inset, where the other parameters are the same as in Figure 1b.

used, and the comparisons between the simulation results of coupled oscillator model and FDTD.

Next, heptamer clusters with another arrangement are investigated, where the gaps of each SNR are along the *x* axis (inset of Figure 10). The extinction spectra with different center SNRs are shown in the main panel of Figure 10. Three Fano resonances are also present in the spectra. The first Fano resonance with the highest energy is red shifting with the increase of *R*, the modulation depth is weak, and there is only a kink when $R < 80$ nm. The modulation depth of the second Fano resonance increases with the increase of *R*, and it shifts to lower energies at the same time. For the third Fano resonance with the lowest energy, there is a blue shifting with the increase of *R*, while the modulation depth increases.

The near-field properties of the superradiant bright mode of the heptamer with new arrangement when $R = 90$ nm are shown in Figure 11a. The overall dipole moment of the whole structure increases with the increase of *R*, which leads to the broadening of the superradiant bright mode. From the near-field distributions of the first Fano resonance as shown in Figure 11b, one can find that the dipole resonances

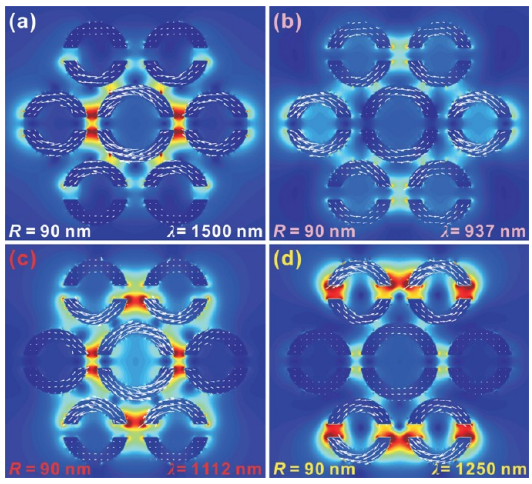

Figure 11. Near-field properties of (a) the superradiant bright mode, (b) the first, (c) the second, and (d) the third Fano resonances when $R = 90$ nm for the heptamer with the new arrangement.

of the middle three SNRs oscillate out of phase, resulting in a cancellation of there dipole moments. Compared to the superradiant bright resonance, there is a weaker radiative damping at this spectral position, leading to the formation of the first Fano resonance. When $R < 80$ nm, the dipole moment of the center SNR is much weaker than that of the left- and right-side SNRs, and the first Fano resonance is not visible in the spectra. It is also found that the plasmons of the upper and lower four SNRs oscillate in phase, which has a strong radiative damping. As a result, the modulation depth of the first Fano resonance is weak. With the increase of *R*, resonance energy of the center SNR is reduced, leading to a red shift of the first Fano resonance. For the second Fano resonance as shown in Figure 11c, the plasmons of the middle three SNRs oscillate in phase, but they are out of phase with the other four SNRs, and the overall dipole moment of the whole structure decreases dramatically at this spectral position, which generates a new subradiant collective mode; its coupling with the superradiant bright mode forms the second Fano resonance. The cancellation of the overall dipole moments becomes more effective with the increase of *R*, and the modulation depth of the second Fano resonance increases. Due to the reduction of the resonance energy of the center SNR, the second Fano resonance also shifts to lower energies with the increase of *R*. By inspecting the near-field distributions of the third Fano resonance as represented in Figure 11d, one can find the quadrupole resonance of SNRs causes the third Fano resonance. But compared to the other kind of heptamer, there is a strong SP coupling between the upper two as well as lower two SNRs, and the resonance energy of the third Fano resonance is less than that of the quadrupole mode. Because of the SP coupling, there is a strong field enhancement between the upper or lower two SNRs,

resulting in additional radiative damping at these areas. The radiative damping is weaker for a larger separation, and the modulation depth of the third Fano resonance increases with the increase of *R*. On the other hand, the SP coupling strength of the upper two as well as lower two SNRs decreases with the increase of *R*, which leads to a blue shift of the third Fano resonance.

The above studies have shown that by the combination of the heptamer and SNR, multiple Fano resonances with strong modulation depths can be obtained, which is very useful for plasmon line shaping. It is also worth noting that we have provided a method to design "plasmonic artificial molecules",[69] which can help to find useful optical responses. The formation of multiple Fano resonances holds true for heptamer clusters composed of other quadrupole supporting structures that have the same optical properties as the SNR. For example, the optical responses of a heptamer cluster composed of nanorod dimers are the same as the heptamer cluster composed of SNRs (Figure S6). For heptamer clusters composed of nanoparticles that have different optical properties as the SNR, optical responses are also different, but other useful properties may be found. For example, the nanocross has a quadrupole mode close to the dipole resonance, but its resonant energy is higher than the dipole mode.[41] When nanocrosses are arranged in a heptamer cluster, very interestingly we observed the formation of magnetic plasmons (Supporting Information, Figure S7), which are useful to design SP waveguiding devices.[65,66]

CONCLUSION

Plasmonic heptamer clusters composed of SNRs are studied in this paper. It is found that there are multiple Fano resonances in the spectra, and the multiple Fano resonances can be switched on and off by adjusting the polarization direction. By inspecting their near-field properties, it is concluded that the first and the third Fano resonances are caused by, respectively, an antibonding and a bonding narrow subradiant resonance. The second Fano resonance is caused by the dark quadrupole mode of the surrounding SNRs. In particular, it is found that the modulation depth as well as the resonance energy of each Fano resonance can be tuned within a wide range by adjusting the structure parameters. By using plasmonic heptamer clusters composed of SNRs, one can modify the plasmon line at several spectral positions simultaneously. This property makes such a structure highly suitable for plasmon line shaping. Recently, optical properties and their applications of the coupled bonding mode as well as the anisotropy effects of NR dimers have been investigated,[70,71] and we expect that plasmonic heptamer clusters composed of SNRs have a high potential to serve as platforms for multiwavelength SERS and biosensing.

METHODS

All spectra presented in this article are calculated using the finite-difference time-domain (FDTD) method.[72] In the simulations, the size of the unit cell is $2 \times 2 \times 2$ nm^3, the complex dielectric constants of gold are taken from measured data,[73] and the surrounding medium is assumed to be water with the refractive index of $n = 1.33$. During the FDTD calculations, an electromagnetic pulse in the wavelength range from 790 to 1667 nm was launched into a box containing the target structure to simulate a propagating plane wave interacting with the nanostructure. The colorscale for the field enhancements is linear, and the colorscale is the same for all panels.

Conflict of Interest: The authors declare no competing financial interest.

Acknowledgment. The authors thank Hui Li for the helpful discussion. This work was supported by the National Natural Science Foundation of China (Grant No. 11104199), and the fund of Taiyuan University of Technology for young teachers.

Supporting Information Available: The extinction spectra of plasmonic heptamer clusters composed of SNRs with different overall size; the calculation results with the coupled oscillator model and the parameters used; and the optical responses of plasmonic heptamer clusters composed of nanorod dimers or nanocrosses. This material is available free of charge *via* the Internet at http://pubs.acs.org.

REFERENCES AND NOTES

1. Maier, S. A. *Plasmonics: Fundamentals and Applications*, 1st ed.; Springer: New York, 2007.
2. Barnes, W. L.; Dereux, A.; Ebbesen, T. W. Surface Plasmon Subwavelength Optics. *Nature* **2003**, *424*, 824–830.
3. Le, F.; Brandl, D. W.; Urzhumov, Y. A.; Wang, H.; Kundu, J.; Halas, N. J.; Aizpurua, J.; Nordlander, P. Metallic Nanoparticle Arrays: A Common Substrate for Both Surface-Enhanced Raman Scattering and Surface-Enhanced Infrared Absorption. *ACS Nano* **2008**, *2*, 707–718.
4. Christ, A.; Martin, O. J. F.; Ekinci, Y.; Gippius, N. A.; Tikhodeev, S. G. Symmetry Breaking in a Plasmonic Metamaterial at Optical Wavelength. *Nano Lett.* **2008**, *8*, 2171–2175.
5. Christ, A.; Ekinci, Y.; Solak, H. H.; Gippius, N. A.; Tikhodeev, S. G.; Martin, O. J. F. Controlling the Fano Interference in a Plasmonic Lattice. *Phys. Rev. B* **2007**, *76*, 201405R.
6. Zhang, S.; Genov, D. A.; Wang, Y.; Liu, M.; Zhang, X. Plasmon-Induced Transparency in Metamaterials. *Phys. Rev. Lett.* **2008**, *101*, 047401.
7. Fano, U. Effects of Configuration Interaction on Intensities and Phase Shifts. *Phys. Rev.* **1961**, *124*, 1866–1878.
8. Verellen, N.; Sonnefraud, Y.; Sobhani, H.; Hao, F.; Moshchalkov, V. V.; Dorpe, P. V.; Nordlander, P.; Maier, S. A. Fano Resonances in Individual Coherent Plasmonic Nanocavities. *Nano Lett.* **2009**, *9*, 1663–1667.
9. Hao, F.; Sonnefraud, Y.; Dorpe, P. V.; Maier, S. A.; Halas, N. J.; Nordlander, P. Symmetry Breaking in Plasmonic Nanocavities: Subradiant LSPR Sensing and a Tunable Fano Resonance. *Nano Lett.* **2008**, *8*, 3983–3988.
10. Verellen, N.; Dorpe, P. V.; Vercruysse, D.; Vandenbosch, G. A. E.; Moshchalkov, V. V. Dark and Bright Localized Surface Plasmons in Nanocrosses. *Opt. Express* **2011**, *19*, 11034–11051.
11. Shao, L.; Fang, C.; Chen, H.; Man, Y. C.; Wang, J.; Lin, H. Q. Distinct Plasmonic Manifestation on Gold Nanorods Induced by the Spatial Perturbation of Small Gold Nanospheres. *Nano Lett.* **2012**, *12*, 1424–1430.
12. Woo, K. C.; Shao, L.; Chen, H.; Liang, Y.; Wang, J.; Lin, H. Q. Universal Scaling and Fano Resonance in the Plasmon

Coupling between Gold Nanorods. *ACS Nano* **2011**, *5*, 5976–5986.
13. Brown, L. V.; Sobhani, H.; Lassiter, J. B.; Nordlander, P.; Halas, N. J. Heterodimers: Plasmonic Properties of Mismatched Nanoparticle Pairs. *ACS Nano* **2010**, *4*, 819–832.
14. Yang, Z. J.; Zhang, Z. S.; Zhang, L. H.; Li, Q. Q.; Hao, Z. H.; Wang, Q. Q. Fano Resonances in Dipole−Quadrupole Plasmon Coupling Nanorod Dimers. *Opt. Lett.* **2011**, *36*, 1542–1544.
15. Bachelier, G.; Russier-Antoine, I.; Benichou, E.; Jonin, C.; Fatti, N. D.; Vallée, F.; Brevet, P. F. Fano Profiles Induced by Near-Field Coupling in Heterogeneous Dimers of Gold and Silver Nanoparticles. *Phys. Rev. Lett.* **2008**, *101*, 197401.
16. Peña-Rodríguez, O.; Pal, U.; Campoy-Quiles, M.; Rodríguez-Fernández, L.; Garriga, M.; Alonso, M. I. Enhanced Fano Resonance in Asymmetrical Au:Ag Heterodimers. *J. Phys. Chem. C* **2011**, *115*, 6410–6414.
17. Yang, Z. J.; Zhang, Z. S.; Zhang, W.; Hao, Z. H.; Wang, Q. Q. Twinned Fano Interferences Induced by Hybridized Plasmons in Au−Ag Nanorod Heterodimers. *Appl. Phys. Lett.* **2010**, *96*, 131113.
18. Fang, Z.; Cai, J.; Yan, Z.; Nordlander, P.; Halas, N. J.; Zhu, X. Removing a Wedge from a Metallic Nanodisk Reveals a Fano Resonance. *Nano Lett.* **2011**, *11*, 4475–4479.
19. Mukherjee, S.; Sobhani, H.; Lassiter, J. B.; Bardhan, R.; Nordlander, P.; Halas, N. J. Fanoshells: Nanoparticles with Built-in Fano Resonances. *Nano Lett.* **2010**, *10*, 2694–2701.
20. Wu, D. J.; Jiang, S. M.; Liu, X. J. Tunable Fano Resonances in Three-Layered Bimetallic Au and Ag Nanoshell. *J. Phys. Chem. C* **2011**, *115*, 23797–23801.
21. Zhang, S.; Bao, K.; Halas, N. J.; Xu, H.; Nordlander, P. Substrate-Induced Fano Resonances of a Plasmonic Nanocube: A Route to Increased-Sensitivity Localized Surface Plasmon Resonance Sensors Revealed. *Nano Lett.* **2011**, *11*, 1657–1663.
22. Chen, H.; Shao, L.; Ming, T.; Woo, K. C.; Man, Y. C.; Wang, J.; Lin, H. Q. Observation of the Fano Resonance in Gold Nanorods Supported on High-Dielectric-Constant Substrates. *ACS Nano* **2011**, *5*, 6754–6763.
23. Spinelli, P.; Lare, C. V.; Verhagen, E.; Polman, A. Controlling Fano Lineshapes in Plasmon-Mediated Light Coupling into a Substrate. *Opt. Express* **2011**, *19*, A303–A311.
24. Fan, J. A.; Wu, C.; Bao, K.; Bao, J.; Bardhan, R.; Halas, N. J; Manoharan, V. N.; Nordlander, P.; Shvets, G.; Capasso, F. Self-Assembled Plasmonic Nanoparticle Clusters. *Science* **2010**, *328*, 1135–1138.
25. Hentschel, M.; Saliba, M.; Vogelgesang, R.; Giessen, H.; Alivisatos, A. P.; Liu, N. Transition from Isolated to Collective Modes in Plasmonic Oligomers. *Nano Lett.* **2010**, *10*, 2721–2726.
26. Frimmer, M.; Coenen, T.; Koenderink, A. F. Signature of a Fano Resonance in a Plasmonic Metamolecule's Local Density of Optical States. *Phys. Rev. Lett.* **2012**, *108*, 077404.
27. Alonso-Gonzalez, P.; Schnell, M.; Sarriugarte, P.; Sobhani, H.; Wu, C.; Arju, N.; Khanikaev, A.; Golmar, F.; Albella, P.; Arzubiaga, L.; *et al*. Real-Space Mapping of Fano Interference in Plasmonic Metamolecules. *Nano Lett.* **2011**, *11*, 3922–3926.
28. Rahmani, M.; Lukiyanchuk, B.; Ng, B.; Tavakkoli, K. G. A.; Liew, T. F.; Hong, M. H. Generation of Pronounced Fano Resonances and Tuning of Subwavelength Spatial Light Distribution in Plasmonic Pentamers. *Opt. Express* **2011**, *19*, 4949–4956.
29. Rahmani, M.; Lukiyanchuk, B.; Nguyen, T. T. V.; Tahmasebi, T.; Lin, Y.; Liew, T. Y. F.; Hong, M. H. Influence of Symmetry Breaking in Pentamers on Fano Resonance and Near-Field Energy Localization. *Opt. Mater. Express* **2011**, *1*, 1409–1415.
30. Fan, J. A.; Bao, K.; Wu, C.; Bao, J.; Bardhan, R.; Halas, N. J.; Manoharan, V. N.; Shvets, G.; Nordlander, P.; Capasso, F. Fano-like Interference in Self-Assembled Plasmonic Quadrumer Clusters. *Nano Lett.* **2010**, *10*, 4680–4685.
31. Rahmani, M.; Lei, D. Y.; Giannini, V.; Lukiyanchuk, B.; Ranjbar, M.; Liew, T. Y. F.; Hong, M.; Maier, S. A. Subgroup Decomposition of Plasmonic Resonances in Hybrid Oligomers: Modeling the Resonance Lineshape. *Nano Lett.* **2012**, *12*, 2101–2106.
32. Rahmani, M.; Tahmasebi, T.; Lin, Y.; Lukiyanchuk, B.; Liew, T. Y. F.; Hong, M. H. Influence of Plasmon Destructive Interferences on Optical Properties of Gold Planar Quadrumers. *Nanotechnology* **2011**, *22*, 245204.
33. Sheikholeslami, S. N.; García-Etxarri, A.; Dionne, J. A. Controlling the Interplay of Electric and Magnetic Modes *via* Fano-like Plasmon Resonances. *Nano Lett.* **2011**, *11*, 3927–3934.
34. Chuntonov, L.; Haran, G. Effect of Symmetry Breaking on the Mode Structure of Trimeric Plasmonic Molecules. *J. Phys. Chem. C* **2011**, *115*, 19488–19495.
35. Lassiter, J. B.; Sobhani, H.; Knight, M. W.; Mielczarek, W. S.; Nordlander, P.; Halas, N. J. Designing and Deconstructing the Fano Lineshape in Plasmonic Nanoclusters. *Nano Lett.* **2012**, *12*, 1058–1062.
36. Cui, Y.; Zhou, J.; Tamma, V. A.; Park, W. Dynamic Tuning and Symmetry Lowering of Fano Resonance in Plasmonic Nanostructure. *ACS Nano* **2012**, *6*, 2385–2393.
37. Lassiter, J. B.; Sobhani, H.; Fan, J. A.; Kundu, J.; Capasso, F.; Nordlander, P.; Halas, N. J. Fano Resonances in Plasmonic Nanoclusters: Geometrical and Chemical Tenability. *Nano Lett.* **2010**, *10*, 3184–3189.
38. Hentschel, M.; Dregely, D.; Vogelgesang, R.; Giessen, H.; Liu, N. Plasmonic Oligomers: The Role of Individual Particles in Collective Behavior. *ACS Nano* **2011**, *5*, 2042–2050.
39. Sonnefraud, Y.; Verellen, N.; Sobhani, H.; Vandenbosch, G. A. E.; Moshchalkov, V. V.; Dorpe, P. V.; Nordlander, P.; Maier, S. A. Experimental Realization of Subradiant, Superradiant, and Fano Resonances in Ring/Disk Plasmonic Nanocavities. *ACS Nano* **2010**, *4*, 1664–1670.
40. Hao, F.; Nordlander, P.; Sonnefraud, Y.; Dorpe, P. V.; Maier, S. A. Tunability of Subradiant Dipolar and Fano-Type Plasmon Resonances in Metallic Ring/Disk Cavities: Implications for Nanoscale Optical Sensing. *ACS Nano* **2009**, *3*, 643–652.
41. Verellen, N.; Dorpe, P. V.; Huang, C.; Lodewijks, K.; Vandenbosch, G. A. E.; Lagae, L.; Moshchalkov, V. V. Plasmon Line Shaping Using Nanocrosses for High Sensitivity Localized Surface Plasmon Resonance Sensing. *Nano Lett.* **2011**, *11*, 391–397.
42. Liu, S. D.; Yang, Z.; Liu, R. P.; Li, X. Y. High Sensitivity Localized Surface Plasmon Resonance Sensing using a Double Split Nanoring Cavity. *J. Phys. Chem. C* **2011**, *115*, 24469–24477.
43. Wu, C.; Khanikaev, A. B.; Adato, R.; Arju, N.; Yanik, A. A.; Altug, H.; Shvets, G. Fano-Resonant Asymmetric Metamaterials for Ultrasensitive Spectroscopy and Identification of Molecular Monolayers. *Nat. Mater.* **2012**, *11*, 69–75.
44. Ye, J.; Wen, F.; Sobhani, H.; Lassiter, J. B.; Dorpe, P. V.; Nordlander, P.; Halas, N. J. Plasmonic Nanoclusters: Near Field Properties of the Fano Resonance Interrogated with SERS. *Nano Lett.* **2012**, *12*, 1660–1667.
45. Ou, F. S.; Hu, M.; Naumov, I.; Kim, A.; Wu, W.; Bratkovsky, A. M.; Li, X.; Williams, R. S.; Li, Z. Hot-Spot Engineering in Polygonal Nanofinger Assemblies for Surface Enhanced Raman Spectroscopy. *Nano Lett.* **2011**, *11*, 2538–2542.
46. Pasquale, A. J.; Reinhard, B. M.; Negro, L. D. Engineering Photonic-Plasmonic Coupling in Metal Nanoparticle Necklaces. *ACS Nano* **2011**, *5*, 6578–6585.
47. Ahn, W.; Boriskina, S. V.; Hong, Y.; Reinhard, B. M. Electromagnetic Field Enhancement and Spectrum Shaping through Plasmonically Integrated Optical Vortices. *Nano Lett.* **2012**, *12*, 219–227.
48. Forestiere, C.; Pasquale, A. J.; Capretti, A.; Miano, G.; Tamburrino, A.; Lee, S. Y.; Reinhard, B. M.; Negro, L. D. Genetically Engineered Plasmonic Nanoarrays. *Nano Lett.* **2012**, *12*, 2037–2044.
49. Zhou, Z. K.; Peng, X. N.; Yang, Z. J.; Zhang, Z. S.; Li, M.; Su, X. R.; Zhang, Q.; Shan, X.; Wang, Q. Q.; Zhang, Z. Tuning Gold Nanorod-Nanoparticle Hybrids into Plasmonic Fano Resonance for Dramatically Enhanced Light Emission and Transmission. *Nano Lett.* **2011**, *11*, 49–55.

50. Liu, H.; Wang, N.; Liu, Y.; Zhao, Y.; Wu, X. Light Transmission Properties of Double-Overlapped Annular Apertures. *Opt. Lett.* **2011**, *36*, 385–387.
51. Taubert, R.; Hentschel, M.; Kästel, J.; Giessen, H. Classical Analog of Electromagnetically Induced Absorption in Plasmonics. *Nano Lett.* **2012**, *12*, 1367–1371.
52. Prodan, E.; Radloff, C.; Halas, N. J.; Nordlander, P. A Hybridization Model for the Plasmon Response of Complex Nanostructures. *Science* **2003**, *302*, 419–422.
53. Joe, Y. S.; Satanin, A. M.; Kim, C. S. Classical Analogy of Fano Resonances. *Phys. Scr.* **2006**, *74*, 259–266.
54. Mirin, N. A.; Bao, K.; Nordlander, P. Fano Resonances in Plasmonic Nanoparticle Aggregates. *J. Phys. Chem. A* **2009**, *113*, 4028–4034.
55. Bao, K.; Mirin, N. A.; Norlander, P. Fano Resonances in Planar Silver Nanosphere Clusters. *Appl. Phys. A: Mater. Sci. Process.* **2010**, *100*, 333–339.
56. Chuntonov, L.; Haran, G. Trimeric Plasmonic Molecules: The Role of Symmetry. *Nano Lett.* **2011**, *11*, 2440–2445.
57. Francescato, Y.; Giannini, V.; Maier, S. A. Plasmonic Systems Unveiled by Fano Resonances. *ACS Nano* **2012**, *6*, 1830–1838.
58. Giannini, V.; Francescato, Y.; Amrania, H.; Phillips, C. C.; Maier, S. A. Fano Resonances in Nanoscale Plasmonic Systems: a Parameter-Free Modeling Approach. *Nano Lett.* **2011**, *11*, 2835–2840.
59. Chen, Y. T.; Chern, R. L.; Lin, H. Y. Multiple Fano Resonances in Metallic Arrays of Asymmetric Dual Stripes. *Appl. Opt.* **2010**, *49*, 2819–2826.
60. Liu, N.; Hentschel, M.; Weiss, T.; Alivisatos, A. P.; Giessen, H. Three-Dimensional Plasmon Rulers. *Science* **2011**, *332*, 1407–1410.
61. Davis, T. J.; Hentschel, M.; Liu, N.; Giessen, H. Analytical Model of the Three-Dimensional Plasmonic Ruler. *ACS Nano* **2012**, *6*, 1291–1298.
62. Artar, A.; Yanik, A. A.; Altug, H. Multispectral Plasmon Induced Transparency in Coupled Meta-atoms. *Nano Lett.* **2011**, *11*, 1685–1689.
63. Artar, A.; Yanik, A. A.; Altug, H. Directional Double Fano Resonances in Plasmonic Hetero-oligomers. *Nano Lett.* **2011**, *11*, 3694–3700.
64. Dregely, D.; Hentschel, M.; Giessen, H. Excitation and Tuning of Higher-Order Fano Resonances in Plasmonic Oligomer Clusters. *ACS Nano* **2011**, *5*, 8202–8211.
65. Liu, N.; Mukherjee, S.; Bao, K.; Brown, L. V.; Dorfmüller, J.; Nordlander, P.; Halas, N. J. Magnetic Plasmon Formation and Propagation in Artificial Aromatic Molecules. *Nano Lett.* **2012**, *12*, 364–369.
66. Liu, N.; Mukherjee, S.; Bao, K.; Li, Y.; Brown, L. V.; Nordlander, P.; Halas, N. J. Manipulating Magnetic Plasmon Propagation in Metallic Nanocluster Networks. *ACS Nano* **2012**, 10.1021/nn301393x.
67. Fu, Y. H.; Zhang, J. B.; Yu, Y. F.; Luk'yanchuk, B. Generating and Manipulating Higher Order Fano Resonances in Dual-Disk Ring Plasmonic Nanostructures. *ACS Nano* **2012**, 10.1021/nn3007898.
68. Jain, P. K.; Eustis, S.; El-Sayed, M. A. Plasmon Coupling in Nanorod Assemblies: Optical Absorption, Discrete Dipole Approximation Simulation, and Exciton-Coupling Model. *J. Phys. Chem. B* **2006**, *110*, 18243–18253.
69. Guerrero-Martínez, A.; Grzelczak, M.; Liz-Marzán, L. M. Molecular Thinking for Nanoplasmonic Design. *ACS Nano* **2012**, *6*, 3655–3662.
70. Tsai, C. Y.; Lin, J. W.; Wu, C. Y.; Lin, P. T.; Lu, T. W.; Lee, P. T. Plasmonic Coupling in Gold Nanoring Dimers: Observation of Coupled Bonding Mode. *Nano Lett.* **2012**, *12*, 1648–1654.
71. Near, R.; Tabor, C.; Duan, J.; Pachter, R.; El-Sayed, M. A. Pronounced Effects of Anisotropy on Plasmonic Properties of Nanorings Fabricated by Electron Beam Lithography. *Nano Lett.* **2012**, *12*, 2158–2164.
72. Taflove, A.; Hagness, S. C. *Computational Electrodynamics: The Finite-Difference Time-Domain Method*; Artech House: Boston, MA, 2005.
73. Johnson, P. B.; Christy, R. W. Optical Constants of Noble Metals. *Phys. Rev. B* **1972**, *6*, 4370.